

# Fluctuations in the formation time of ultracold dimers from fermionic atoms

H. Uys, T. Miyakawa, D. Meiser, and P. Meystre

*Optical Sciences Center and Department of Physics  
The University of Arizona, Tucson, AZ 85721*

(Dated: July 3, 2018)

We investigate the temporal fluctuations characteristic of the formation of molecular dimers from ultracold fermionic atoms via Raman photoassociation. The quantum fluctuations inherent to the initial atomic state result in large fluctuations in the passage time from atoms to molecules. Assuming degeneracy of kinetic energies of atoms in the strong coupling limit we find that a heuristic classical stochastic model yields qualitative agreement with the full quantum treatment in the initial stages of the dynamics. We also show that in contrast to the association of atoms into dimers, the reverse process of dissociation from a condensate of bosonic dimers exhibits little passage time fluctuations. Finally we explore effects due to the non-degeneracy of atomic kinetic energies.

PACS numbers: 03.75.Lm, 03.75.Ss, 42.50.Ar

## I. INTRODUCTION

The coherent formation of ultracold diatomic molecules from quantum-degenerate bosonic or fermionic atomic gases, via either Feshbach resonances [1] or two-photon Raman photoassociation [2], has witnessed spectacular developments in recent years and has led to the first realization of molecular condensates [3]. Because in these experiments the molecular field is initially in a vacuum state, it is to be expected that quantum fluctuations play a dominant role in the early stages of molecule formation. These fluctuations manifest themselves in the quantum statistics of the resulting molecular field, and also in the time that it takes for the number of generated molecules to reach a specific value, the so-called passage time statistics. This problem is closely related to other situations where quantum (or thermal) fluctuations trigger a system to undergo a transition away from a dynamically unstable state. One such example familiar from quantum optics is superradiance [4] (or strictly speaking superfluorescence), a situation where an ensemble of two-level systems initially in their excited electronic state and coupled to the electromagnetic field vacuum undergoes a transition characterized by the emission of an intense light pulse. One important difference is that in superfluorescence experiments the atoms are normally coupled to a continuum of modes of the radiation field, practically leading to an irreversible decay to their ground state, while in the problem at hand the molecular field is to a good approximation single-mode, leading to reversible dynamics.

One important way to characterize the dynamics of molecule formation is by way of the so-called passage time, which is defined as the time it takes to produce a predetermined number of molecules. The goal of this paper is to study the passage time statistics resulting from the initial quantum fluctuations of the atomic matter-wave field. We also compare this situation with the dynamics of dissociation of a molecular condensate into fermionic atomic pairs, showing significant qualitative differences between the two cases.

The paper is organized as follows: Section II establishes our notation, presents our model, and shows that the application of an Anderson mapping [5] leads to the description of photoassociation of fermions in terms of the inhomogeneously broadened Tavis-Cummings model of quantum optics. Section III concentrates on a “homogeneously broadened” version of this model that neglects the spread in fermion energies, an approximation shown to be valid for sufficiently small numbers of atoms. There we also discuss an approximate stochastic classical description [6, 7] that yields a satisfactory qualitative agreement with the full quantum results for short enough times. This section concludes by comparing the passage time statistics associated with photoassociation and the reverse process of photodissociation. The results of a numerical analysis of the full, inhomogeneously broadened model are presented in section IV. Finally section V is a summary and outlook.

## II. THE MODEL

In typical experiments that produce molecules via Feshbach resonance the magnetic field is swept across the resonance. In the strong coupling regime  $k_F a \geq 1$  in the vicinity of the resonance, where  $k_F$  is the Fermi wave number and  $a$  is the s-wave scattering length, the interpretation of the molecular state is subject to conceptual difficulties stemming from the dressing of the “bare” molecular state by atom pairs in the open channel [8]. Furthermore, since the binding energy of the molecules is very small, of the order  $10^{-11}$ eV, they are larger than the interatomic separation. Another consequence of the almost vanishing binding energy is that nearly every time-dependent process becomes nonadiabatic with respect to the time scale set by the inverse of the binding energy. To avoid these difficulties we restrict our considerations in this paper to the description of a quantum-degenerate gas of fermionic atoms of mass  $m_f$  and spin  $\alpha = \uparrow, \downarrow$ , coupled coherently to bosonic molecules of mass  $m_b = 2m_f$  and zero momentum via *photoassociation* rather than Fesh-

bach resonance.

Neglecting collisions between fermions and assuming that for short enough times the molecules can be described by a single-mode bosonic field, this system can be described by the boson-fermion model Hamiltonian

$$H = \sum_k \frac{1}{2} \hbar \omega_k \left( \hat{c}_{k\uparrow}^\dagger \hat{c}_{k\uparrow} + \hat{c}_{-k\downarrow}^\dagger \hat{c}_{-k\downarrow} \right) + \hbar \omega_b \hat{b}^\dagger \hat{b} + \hbar \chi \sum_k \left( \hat{b}^\dagger \hat{c}_{k\uparrow} \hat{c}_{-k\downarrow} + \hat{b} \hat{c}_{-k\downarrow}^\dagger \hat{c}_{k\uparrow}^\dagger \right), \quad (1)$$

where  $\hat{b}^\dagger, \hat{b}$  are molecular bosonic creation and annihilation operators and  $\hat{c}_{k\alpha}^\dagger, \hat{c}_{k\alpha}$  are fermionic creation and annihilation operators describing atoms of momentum  $\hbar k$  and spin  $\alpha$ . The first and second terms in Eq. (1) describe the energy,  $\omega_k = \hbar^2 k^2 / m_f$ , of the atoms, and the detuning energy of the molecules respectively, and the third term describes the photoassociation of pairs of atoms of opposite momentum into molecules.

Introducing the pseudo-spin operators [5]

$$\begin{aligned} \hat{\sigma}_k^z &= \frac{1}{2} (\hat{c}_{k\uparrow}^\dagger \hat{c}_{k\uparrow} + \hat{c}_{-k\downarrow}^\dagger \hat{c}_{-k\downarrow} - 1), \\ \hat{\sigma}_k^+ &= (\hat{\sigma}_k^-)^\dagger = \hat{c}_{-k\downarrow}^\dagger \hat{c}_{k\uparrow}, \end{aligned} \quad (2)$$

which are easily seen to obey the SU(2) commutation relations

$$[\hat{\sigma}_k^+, \hat{\sigma}_{k'}^-] = 2\delta_{kk'} \hat{\sigma}_k^z \quad (3)$$

$$[\hat{\sigma}_k^z, \hat{\sigma}_{k'}^\pm] = \pm \delta_{kk'} \hat{\sigma}_k^\pm, \quad (4)$$

where  $\delta_{kk'}$  is the Kronecker delta function, the Hamiltonian (1) becomes, within an unimportant constant [9, 10],

$$H = \sum_k \hbar \omega_k \hat{\sigma}_k^z + \hbar \omega_b \hat{b}^\dagger \hat{b} + \hbar \chi \sum_k \left( \hat{b}^\dagger \hat{\sigma}_k^- + \hat{b} \hat{\sigma}_k^+ \right). \quad (5)$$

This Hamiltonian is known in quantum optics as the inhomogeneously broadened (or non-degenerate) Tavis-Cummings model [11]. It describes the coupling of an ensemble of two-level atoms to a single-mode electromagnetic field. Hence the mapping (2) establishes the formal analogy between the problem at hand and Dicke superradiance, with the caveat already mentioned that we are dealing with a single bosonic mode [9, 10, 12, 13, 14, 15]. Instead of real two-level atoms, pairs of fermionic atoms are now described as effective two-level systems whose ground state corresponds to the absence of a pair,  $|g_k\rangle = |0_{k\uparrow}, 0_{-k\downarrow}\rangle$  and the excited state to a pair of atoms of opposite momenta,  $|e_k\rangle = |1_{k\uparrow}, 1_{-k\downarrow}\rangle$ .

The initial condition of the superradiance problem is a sample of inverted two-level atoms. It corresponds in the present case to the initial atomic state

$$|F\rangle = \prod_k \hat{\sigma}_k^+ |0\rangle, \quad (6)$$

where the product is taken up to the Fermi surface for  $T = 0$ , while the molecular field is in the vacuum state

$|0\rangle$ . We concentrate in the following on times short enough that the atomic sample remains essentially undepleted and it is sufficient to consider only fermionic levels up to the Fermi surface in Eq. (5).

### III. DEGENERATE MODEL

We consider first the simplified situation of a degenerate model in which the inhomogeneous broadening due to the spread in atomic kinetic energies is ignored. This is justified provided that these energies are small compared to the atom-molecule coupling energy,  $\beta = \epsilon_F / (\hbar \chi) \ll 1$ , where  $\epsilon_F$  is the Fermi energy. This approximation is the analog of the homogeneous broadening limit of quantum optics, and of the Raman-Nath approximation in atomic diffraction. As we will find it is valid only for relatively small ( $\sim 10^2 - 10^3$ ) particle numbers, but the model exhibits the essential physics.

The atom-molecule coupling has been estimated [19, 20] for the case of  $^{87}\text{Rb}$  to be  $\chi \sqrt{V} \approx 7.6 \times 10^{-7} \text{ m}^{3/2} \text{ s}^{-1}$ , so that  $\beta = \epsilon_F / \hbar \chi \approx 10^{-2} N^{7/12}$ . In the last term we have related the Fermi energy and volume to the oscillator frequency  $\omega_{\text{ho}}$  of a spherically symmetric harmonic trap via  $\epsilon_F \approx N^{1/3} \hbar \omega_{\text{ho}}$  and  $V \approx N^{1/2} a_{\text{osc}}^3$  where  $a_{\text{osc}} = \sqrt{\hbar / m \omega_{\text{ho}}}$  is the oscillator length. Typical experiments use traps with  $\omega_{\text{ho}} \approx 100 \text{ Hz}$ . In the case of  $^{87}\text{Rb}$  the trap should contain at most  $\sim 10^2 - 10^3$  atom pairs to be in this regime, i.e. to have  $\beta \lesssim 1$ . For larger samples, it is necessary to account for the inhomogeneous broadening of the sample, a situation that we consider in the next section. For any atom numbers, the characteristic time scale is given  $\tau_p = 1 / \chi \sqrt{N} \simeq 5.8 \times 10^{-3} N^{-1/4} \text{ s}$  for parameters used in this paper.

#### A. Quantum description

Limiting for now our considerations to small atomic samples, we approximate all  $\omega_k$ 's by  $\omega_F$  and introduce the collective pseudo-spin operators

$$\begin{aligned} \hat{S}_z &= \sum_k \hat{\sigma}_k^z, \\ \hat{S}^\pm &= \sum_k \hat{\sigma}_k^\pm, \end{aligned} \quad (7)$$

which again obey SU(2) commutation relations, yielding the standard Tavis-Cummings Hamiltonian [11, 15]

$$H = \hbar \omega_F \hat{S}_z + \hbar \omega_b \hat{b}^\dagger \hat{b} + \hbar \chi (\hat{b} \hat{S}^+ + \hat{b}^\dagger \hat{S}^-). \quad (8)$$

This Hamiltonian conserves the total spin operator  $\hat{S}^2$ , which, by using the pseudo-spin commutation relations, can be expressed as

$$\hat{S}^2 = \hat{S}^+ \hat{S}^- + \hat{S}_z (\hat{S}_z - 1), \quad (9)$$

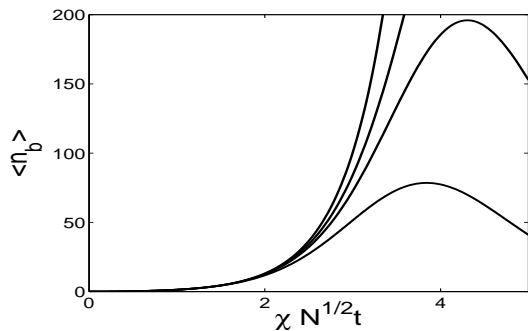


FIG. 1: Short-time dynamics of  $\langle \hat{n}_b \rangle$ . From left to right, the curves give the linearized solution (21) and the full quantum results for  $N = 500$ ,  $N = 250$ , and  $N = 100$ , respectively.

with

$$\hat{S}^2|F\rangle = S(S+1)|F\rangle = \frac{N}{2} \left( \frac{N}{2} + 1 \right) |F\rangle, \quad (10)$$

so that  $S = N/2$ . Here

$$N = \hat{b}^\dagger \hat{b} + \sum_k (\hat{c}_{k\uparrow}^\dagger \hat{c}_{k\uparrow} + \hat{c}_{-k\downarrow}^\dagger \hat{c}_{-k\downarrow})/2 = \hat{n}_b + \hat{n}_p \quad (11)$$

is the total number of molecules and atomic pairs, which is conserved by the Hamiltonian (1). From the definition of  $S_z$  we also have that

$$\hat{S}_z = \frac{1}{2}(2\hat{n}_p - N) = \frac{N}{2} - \hat{n}_b = \frac{1}{2}(\hat{n}_p - \hat{n}_b), \quad (12)$$

hence  $\hat{S}_z$  measures the difference in the numbers of atom pairs and molecules.

Introducing for convenience the joint coherence operators

$$\begin{aligned} \hat{J}_x &= (\hat{b}\hat{S}^+ + \hat{b}^\dagger\hat{S}^-)/2, \\ \hat{J}_y &= (\hat{b}\hat{S}^+ - \hat{b}^\dagger\hat{S}^-)/2i, \end{aligned} \quad (13)$$

yields the Heisenberg equations of motion

$$\dot{\hat{n}}_b = -2\chi\hat{J}_y, \quad (14)$$

$$\dot{\hat{J}}_x = \delta\hat{J}_y \quad (15)$$

$$\dot{\hat{J}}_y = -\delta\hat{J}_x - \chi(2\hat{S}_z\hat{n}_b + \hat{S}^+\hat{S}^-), \quad (16)$$

where  $\delta = \omega_b - \omega_F$ , so that  $2\chi\hat{J}_x + \delta\hat{n}_b$  is a constant of motion.

In the following, we confine our discussion to the case of  $\delta = 0$  for simplicity. We thus neglect the contribution of  $J_x$  in Eq. (16). In order to obtain an analytical solution valid for short times for  $\langle \hat{n}_b \rangle$ , where  $\langle \rangle$  indicates the expectation value, and assuming the initial state  $|F\rangle$ , we keep only terms of order  $\hat{n}_b$  on the right in Eq. (16). Using Eqs. (9) and (12), we reexpress  $\hat{S}^+\hat{S}^-$  as

$$\hat{S}^+\hat{S}^- = -\hat{n}_b^2 + (2S-1)\hat{n}_b + \hat{\zeta}^+\hat{\zeta}^-, \quad (17)$$

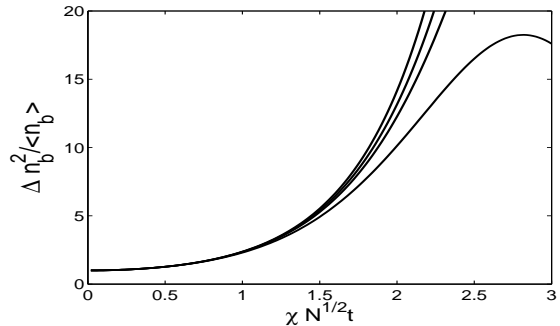


FIG. 2: Short time dynamics for  $\Delta n_b^2 / \langle \hat{n}_b \rangle$ . From left to right, the four curves give the linearized solution (22) and the full quantum results for  $N = 500$ ,  $N = 250$ , and  $N = 100$  respectively.

where we have introduced for convenience the operator

$$\hat{\zeta}^+\hat{\zeta}^- = \hat{S}^2 - S(S-1). \quad (18)$$

Substituting then Eq. (17) into Eq. (16) and dropping the term proportional to  $\hat{n}_b^2$ , we have for the early stages of molecule formation

$$\dot{\hat{J}}_y \approx -2\chi N \hat{n}_b - \chi \hat{\zeta}^+\hat{\zeta}^-. \quad (19)$$

Differentiating Eq. (14), taking its expectation value, and substituting Eq. (19) into the resulting form yields

$$\ddot{\hat{n}}_b \approx \chi^2 (4N\hat{n}_b + 2\hat{\zeta}^+\hat{\zeta}^-) \quad (20)$$

For the initial state  $|F\rangle$  this has the solution

$$\langle \hat{n}_b(t) \rangle \approx \left( \langle \hat{\zeta}^+\hat{\zeta}^- \rangle / N \right) \sinh^2(\chi\sqrt{N}t). \quad (21)$$

Similarly, the variance of the molecule number distribution is found to be

$$\begin{aligned} \Delta n_b^2(t) &= \langle \hat{n}_b^2(t) \rangle - \langle \hat{n}_b(t) \rangle^2 \\ &\approx \left( \langle \hat{\zeta}^+\hat{\zeta}^- \rangle / 8N \right) \left( \cosh(4\chi\sqrt{N}t) - 1 \right). \end{aligned} \quad (22)$$

Figure 1 compares the average molecule number  $\langle \hat{n}_b \rangle$  and Fig. 2 the normalized variance  $\Delta n_b^2 / \langle \hat{n}_b \rangle$  from Eqs. (21) and (22) respectively, with the full quantum solution obtained by direct diagonalization of the Hamiltonian (8). Both approaches agree within 5% until about 20% of the population of atom pairs has been converted into molecules. Note that

$$\lim_{\chi\sqrt{N}t \rightarrow 0} \Delta n_b^2 / \langle \hat{n}_b \rangle = 1. \quad (23)$$

This is indicative of the fact that for short times the molecule field is thermal in character, see for example [10] and references therein. This is further confirmed by a comparison of the molecular number statistics to a thermal distribution, as illustrated in Fig. 3.

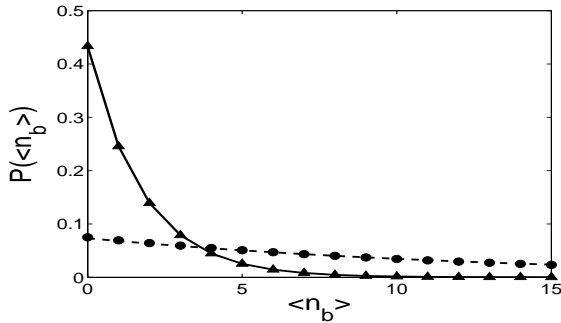


FIG. 3: Molecule number statistics at  $\chi\sqrt{N}t = 1.0$ : solid line - full quantum result, triangles - thermal distribution, and  $\chi\sqrt{N}t = 2.0$ : dashed line - full quantum result, circles - thermal distribution, for  $N = 500$ .

### B. Classical stochastic description

Eq.(19) shows that for the initial state  $|F\rangle$  the source of the molecular field is the operator  $\hat{\zeta}^+\hat{\zeta}^-$ . This is the non-vanishing part of the second-order moment  $\langle \hat{S}^+\hat{S}^- \rangle$ , which is a measure of fluctuations of the atomic field. Since the molecular field is initially in a vacuum, its growth is therefore triggered solely by these quantum fluctuations.

It is oftentimes possible to simulate the effects of quantum fluctuations by averaging over a large number of classical trajectories triggered by random noise. To implement such an approach, we first observe that for  $N \gg 1$  the higher-order moments of the pseudo-spin operators  $\hat{S}^\pm$  factorize approximately into a sum of products of second-order moments [16, 17], e.g.,

$$\langle \hat{S}^+\hat{S}^+\hat{S}^-\hat{S}^- \rangle = 2\langle \hat{S}^+\hat{S}^- \rangle \langle \hat{S}^+\hat{S}^- \rangle + O(S^{-1}). \quad (24)$$

We then proceed by replacing the quantum operator  $\hat{S}^+$  by a stochastic classical variable  $s^+$  and assuming that its fluctuations obey random Gaussian statistics, the probability distribution of  $s^+$  being given by

$$p(s^+) = \frac{1}{\sqrt{2\pi}\Delta\hat{S}^+} \exp\left[-|s^+|^2/2(\Delta\hat{S}^+)^2\right] \quad (25)$$

where the variance  $(\Delta\hat{S}^+)^2$  is adjusted to its quantum value

$$(\Delta\hat{S}^+)^2 = \langle |\hat{S}^+|^2 \rangle - \langle \hat{S}^+ \rangle^2 = N \quad (26)$$

for the initial state  $|F\rangle$ .

The resulting passage time statistics  $\rho(\tau)$  can be determined numerically by first obtaining classical trajectories for  $\langle \hat{n}_b(t) \rangle$  using Eq. (21) and assuming that the initial values of  $s^+$  follow the distribution (25). Taking into account that each choice of  $|s^+|^2$  within a differential element  $ds^+$  maps  $\langle \hat{n}_b(t) \rangle$  in such a way that it reaches a fixed reference value  $n_b^{\text{ref}}$  after a uniquely determined

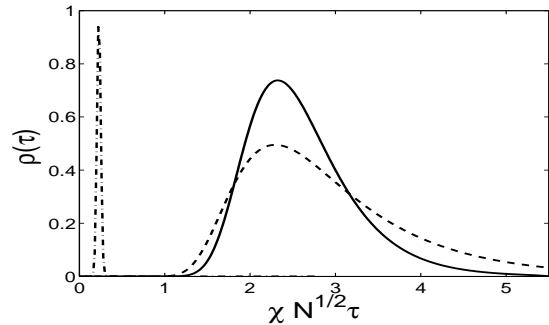


FIG. 4: Passage time distribution for converting 5% of the initial population consisting of only atoms (molecules) into molecules (atoms) for  $N = 500$ . For initially all atoms: solid line - full quantum description; dashed line - classical stochastic model. For initially all molecules: dot-dashed line - full quantum result

passage time  $\tau$  within the differential element  $d\tau$ , it follows that the probability of a particular value of  $s^+$  is equal to the probability of measuring  $\langle \hat{n}_b \rangle = n_b^{\text{ref}}$  at that time  $\tau$

$$|p(s^+)| ds^+(\tau, n_b^{\text{ref}}) = \rho(\tau) d\tau = |p(s^+(\tau))f(\tau, n_b^{\text{ref}})| d\tau, \quad (27)$$

the differential elements  $ds^+$  and  $d\tau$  being related by

$$f(\tau, n_b^{\text{ref}}) = |ds^+(\tau, n_b^{\text{ref}})/d\tau|. \quad (28)$$

By fixing  $\langle \hat{n}_b(\tau) \rangle = n_b^{\text{ref}}$  one can invert Eq. (21) which upon differentiation with respect to  $\tau$  gives

$$f(\tau, n_b^{\text{ref}}) = \chi N \sqrt{n_b^{\text{ref}}} \frac{\cosh(\chi\sqrt{N}\tau)}{\sinh^2(\chi\sqrt{N}\tau)}. \quad (29)$$

We thus obtain an analytical expression for the passage time distribution  $\rho(\tau)$  as

$$\rho(\tau) = \left( \chi \sqrt{\frac{2n_b^{\text{ref}}N}{\pi}} \right) \frac{\cosh(\chi\sqrt{N}\tau)}{\sinh^2(\chi\sqrt{N}\tau)} \times \exp\left(-\frac{n_b^{\text{ref}}}{2\sinh^2(\chi\sqrt{N}\tau)}\right). \quad (30)$$

The dashed line in Fig. 4, obtained from Eq. (30), shows the distribution of passage times required to produce a normalized molecule number  $n_b^{\text{ref}}/N = 0.05$  from a sample initially containing  $N = 500$  pairs of atomic fermions. It should be compared to the solid line, which is the result of the full quantum dynamics. The classical result reproduces qualitatively the broad and asymmetric distribution of the quantum solution. However, it does not reproduce well the leading and trailing edges of the distribution, which depend on the higher order moments of the classical field  $s^+$  and are poorly treated by the assumption of Gaussian noise. In addition the continuous

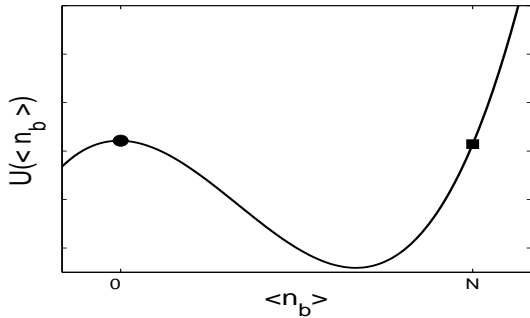


FIG. 5: Effective potential for a system with  $N \gg 1$ . The circle (square) corresponds to an initial state with all fermionic atoms (molecules). The part of the potential for  $n_b < 0$  is unphysical.

distribution of the classical model fails to properly describe the dynamics of the system at very low molecule numbers when the discrete nature of molecule number is more important.

### C. Photodissociation

The passage time distribution for the photoassociation of fermionic atoms into molecules differs sharply from its counterpart for the reverse process of photodissociation from a molecular condensate into fermionic atom pairs, which is plotted as the dot-dashed line in Fig. 4. In contrast to photoassociation, this latter process suffers significantly reduced fluctuations. One can gain an intuitive understanding of this difference by treating the short-time molecular population classically,  $\langle \hat{n}_b \rangle \rightarrow n_b$ . Within this approximation, the Heisenberg equations of motion (14)-(15) can be recast in the form of a Newton equation [15]

$$\frac{d^2 n_b}{dt^2} = -\frac{dU(n_b)}{dn_b}, \quad (31)$$

where the effective potential  $U(n_b)$  is given by

$$U(n_b) = \frac{1}{4}N^2(N+3) - 2Nn_b - (2N-1)n_b^2 + 2n_b^3 \quad (32)$$

and is cubic in  $n_b$ , see Fig. 5.

In case the system is initially composed solely of fermionic atoms,  $n_b(0) = 0$ , the initial state is dynamically unstable, with fluctuations having a large impact in the build-up of  $n_b$ . In contrast, when it consists initially solely of molecules,  $n_b = N$ , the initial state is far from the point of unstable equilibrium, and  $n_b$  simply “rolls down” the potential in a manner largely insensitive to quantum fluctuations. This is a consequence of the fact that the bosonic initial state provides a mean field that is more amenable to a classical description.

## IV. NON-DEGENERATE MODEL

Although the degenerate model offers the benefit of allowing analytical solutions and an intuitive physical interpretation in the short time limit, we have seen that it is only valid for relatively modest values of  $N$ . Current experiments, however, generally trap  $\sim 10^5 - 10^6$  atoms, in which case it is important to properly account for the atomic kinetic energies within the Fermi sea.

From the Hamiltonian (5), we readily obtain the Heisenberg equations of motion:

$$\frac{d\hat{n}_b}{dt} = -2\chi \sum_k \hat{j}_k^y, \quad (33)$$

$$\frac{d\hat{j}_k^x}{dt} = \delta_k \hat{j}_k^y, \quad (34)$$

$$\begin{aligned} \frac{d\hat{j}_k^y}{dt} &= -\delta_k \hat{j}_k^x - 2\chi \hat{n}_b \hat{\sigma}_k^z - \frac{1}{2}\chi \sum_{k'} (\hat{\sigma}_k^+ \hat{\sigma}_{k'}^- + \hat{\sigma}_{k'}^+ \hat{\sigma}_k^-) \\ &\approx -\delta_k \hat{j}_k^x - 2\chi \hat{n}_b \hat{\sigma}_k^z - \chi \hat{\sigma}_k^+ \hat{\sigma}_k^-, \end{aligned} \quad (35)$$

where we have defined

$$\hat{j}_k^x = \frac{\hat{b}\hat{\sigma}_k^+ + \hat{b}^\dagger\hat{\sigma}_k^-}{2}, \quad (36)$$

$$\hat{j}_k^y = \frac{\hat{b}\hat{\sigma}_k^+ - \hat{b}^\dagger\hat{\sigma}_k^-}{2i}, \quad (37)$$

and  $\delta_k = \omega_b - \omega_k^f$ . In Eq. (35) we have also made the approximation

$$\hat{\sigma}_{k'}^+ \hat{\sigma}_k^- \approx \delta_{kk'} \hat{\sigma}_{k'}^+ \hat{\sigma}_k^-, \quad (38)$$

which is valid for short times when starting from the initial state  $|F\rangle$ . In order to develop a classical model in analogy with the degenerate case we define

$$\hat{n}_k^b = 1 - \frac{1}{2} \left( \hat{c}_k^\dagger \hat{c}_k + \hat{c}_{-k}^\dagger \hat{c}_{-k} \right). \quad (39)$$

Since  $\sum_k \langle \hat{n}_k^b \rangle = \langle \hat{n}_b \rangle$ , where the sum runs over momenta inside the Fermi sea, the expectation value of this operator can be interpreted as that fraction of the initial pair of atoms of momenta  $(-k, k)$  that has been converted into a molecule. Note that

$$\hat{\sigma}_k^2 = \hat{\sigma}_k^+ \hat{\sigma}_k^- + \hat{\sigma}_k^z (\hat{\sigma}_k^z - 1) \quad (40)$$

with  $\hat{\sigma}_k^2 |F\rangle = \frac{1}{2}(\frac{1}{2} + 1)|F\rangle$  and

$$\hat{\sigma}_k^z = \frac{1}{2} - \hat{n}_k^b, \quad (41)$$

so

$$\begin{aligned} \hat{\sigma}_k^+ \hat{\sigma}_k^- &= \hat{\sigma}_k^2 - \hat{\sigma}_k^z (\hat{\sigma}_k^z - 1) \\ &= -(\hat{n}_k^b)^2 + \hat{\zeta}_k^+ \hat{\zeta}_k^-, \end{aligned} \quad (42)$$

where we have defined

$$\hat{\zeta}_k^+ \hat{\zeta}_k^- = \hat{\sigma}_k^2 - \frac{1}{2}(\frac{1}{2} - 1). \quad (43)$$

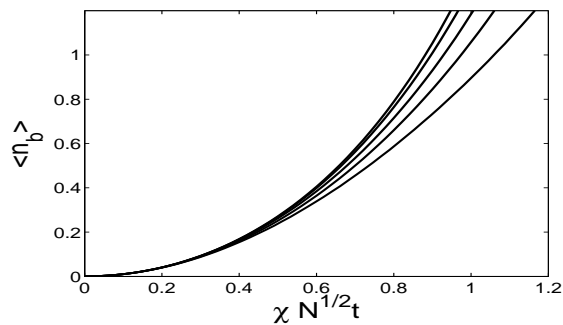


FIG. 6: Average molecule number as a function of time for various values of the coupling strength. From left to right: degenerate analytical, full quantum treatment for  $\beta = 0.1$ ; short-time treatment for  $\beta = 0.1$ , short-time treatment for  $\beta = 10$ , full quantum treatment for  $\beta = 10$ . In this example we used  $N = 18$ .

Finally, by substituting Eqs. (42) and (41) into Eq. (33) we obtain

$$\frac{d\hat{j}_k^y}{dt} \approx -\delta_k \hat{j}_k^x - \chi \hat{n}_b - \chi \hat{\zeta}_k^+ \hat{\zeta}_k^- . \quad (44)$$

Short time results were obtained by integrating Eqs. (33), (34) and (44) numerically using a fourth order Runge-Kutta procedure. Those numerical simulations should reproduce the degenerate model in the limit  $\beta \ll 1$ . Note however that the short-time approximation (38) is slightly different from that made in order to obtain Eq.(19). In particular, Eq. (38) ignores a contribution linear in  $\hat{n}_b$  and as a consequence  $\langle \hat{n}_b \rangle$  increases more slowly in the approximate non-degenerate simulation so that for small  $\beta$  it agrees only within  $\sim 10\%$  with the degenerate model once 5% of the initial population of atom pairs has been converted into molecules. This is illustrated in Fig. 6 which plots the average molecule number as a function of time.

Although calculations with larger particle number are computationally tractable for short times, we have restricted our calculations to 18 atom pairs in order to allow an exact numerical treatment of the full quantum

non-degenerate model. Figure 6 shows from left to right the degenerate analytical solution (21), the full quantum result with  $\beta = 0.1$ , the short time result with  $\beta = 0.1$ , short time result with  $\beta = 10$  and the full quantum result for  $\beta = 10$ , respectively. The full quantum result with  $\beta = 0.1$  is indistinguishable from the full quantum treatment in the degenerate model, as expected. These simulations illustrate in particular that the formation of molecules is suppressed for increased  $\beta$ . This is a consequence of the fact that a significant fraction of the atom pairs are detuned from resonance and therefore converted more slowly and incompletely into molecules.

## V. SUMMARY AND OUTLOOK

We have shown that the early stages of molecular dimer formation from fermionic atoms are characterized by large fluctuations that reflect the quantum fluctuations in the initial atomic state. In contrast, the reverse process of dissociation of a condensate of molecular dimers is largely deterministic. The reason for this asymmetry can be traced to the fact that in contrast to a quantum-degenerate fermionic system, the initial state of the molecular condensate is well described by a mean-field theory, that is, it is largely classical and relatively devoid of quantum fluctuations.

As long as the atom-molecule coupling is dominant,  $\beta \ll 1$ , the kinetic energies are unimportant and a degenerate model can accurately describe the molecule formation. This is confirmed by our numerical simulations which show that the results of the degenerate model and the full quantum results are indistinguishable for  $\beta \lesssim 0.1$ . Small deviations appear for  $\beta \approx 1$ , and the creation of molecules is dramatically suppressed for higher ratios.

Future work will extend these considerations to a more realistic multimode description of the association process as well as a more detailed description of the two-body physics, which should in particular include the dressing of molecules by the open channel atomic pairs that is important in Feshbach sweeps. We will also extend our model to the case of fermionic molecules.

This work is supported in part by the US Office of Naval Research, the NSF, the US Army Research Office, NASA, and the Joint Services Optics Program.

- 
- [1] S. Inouye, M. R. Andrews, J. Stenger, H.-J. Miesner, D. M. Stamper-Kurn, and W. Ketterle, *Nature* (London) **392**, 151 (1998).
  - [2] R. Wynar, R. S. Freeland, D. J. Han, C. Ryu, and D. J. Heinzen, *Science* **287**, 1016 (2000).
  - [3] M. Greiner, C. A. Regal, and D. S. Jin, *Nature* (London) **426**, 537 (2003); M. W. Zwierlein *et al.*, *Phys. Rev. Lett.* **91**, 250401 (2003); S. Jochim *et al.*, *Science* **301**, 2101 (2003).
  - [4] R.H. Dicke, *Phys. Rev.* **93**, 99 (1954).
  - [5] P.W. Anderson, *Phys. Rev.* **112**, 1900 (1958).
  - [6] F. Haake, H. King, G. Schröder, J. W. Haus, and R. J. Glauber, *Phys. Rev. A* **20**, 2047 (1979).
  - [7] F. Haake, J. W. Haus, H. King, G. Schröder, and R. J. Glauber, *Phys. Rev. A* **23**, 1322 (1981).
  - [8] This is discussed in particular by K. Goral *et al.*, *J. Phys. B* **37**, 3457 (2004) for the case of bosonic atoms and by G.M. Bruun and C.J. Pethick, *Phys. Rev. Lett.* **92**, 140404 (2004) for the case of fermions.
  - [9] R. A. Barankov and L. S. Levitov, *Phys. Rev. Lett.* **93**, 130403 (2004).
  - [10] D. Meiser and P. Meystre, *Phys. Rev. Lett.* **94**, 093001 (2005).
  - [11] M. Tavis and F. W. Cummings, *Phys. Rev.* **170**, 379

- (1968).
- [12] J. Javanainen *et al.*, Phys. Rev. Lett. **92**, 200402 (2004).
- [13] A. V. Andreev, V. Gurarie, and L. Radzihovsky, Phys. Rev. Lett. **93**, 130402 (2004).
- [14] I. Tikhonenkov and A. Vardi, cond-mat/0407424.
- [15] T. Miyakawa and P. Meystre, Phys. Rev. A **71**, 033624 (2005).
- [16] I.S. Reed, IRE Trans. of Info. Th. **8** (3), 194 (1962).
- [17] L. Mandel and E. Wolf, *Optical Coherence and Quantum Optics* (Cambridge University Press, 1995).
- [18] G. M. Falco and H. T. Stoof, Phys. Rev. Lett. **92**, 130401 (2004).
- [19] D. J. Heinzen, R. Wynar, P. D. Drummond, and K. V. Kheruntsyan, Phys. Rev. Lett. **84**, 5029 (2000).
- [20] Although  $^{87}\text{Rb}$  is bosonic, its statistical nature does not enter in the calculation of coupling strength so that it gives an adequate order of magnitude estimate.